

SIMULATION OF INTERPHASE EXCHANGE IN HETEROGENEOUS MEDIA TO DEVELOP HIGHLY EFFICIENT TECHNOLOGIES

Yu. V. Polezhaev, D. S. Mikhatulin, and P. V. Nikitin

UDC 629.7.018.3:620.193.1+629.7.067

Continuous-medium flows containing suspended particles have drawn the attention of research workers for several decades now. Experiments have shown that even a small amount of admixture in the form of solid particles may exert a substantial influence on the hydrodynamics and convective heat exchange of a stream. Insight into the physics of the interaction of particles with the carrier phase and bodies immersed in the stream makes it possible to control the stream for the purpose of creating fundamentally new technologies for the synthesis and treatment of materials. This is due primarily to the fact that the presence of a disperse admixture in a continuous-medium flow considerably intensifies the processes of transfer and exchange of momentum and heat.

1. Fundamental Investigations of the Thermal and Force Effect of Heterogeneous Streams on Barriers.

From the standpoint of the mechanics of liquids and gases heterogeneous streams possess a variety of fundamental differences from a stream of a single-phase medium. For example, often the trajectory of the motion of the particles does not coincide with the carrier-phase streamlines, while the velocity of the particles may both be lower or higher than the gas-component velocity. Therefore, the classical model of a continuous medium is unsuitable for the description of heterogeneous media. Experimental investigation of convective heat exchange in heterogeneous streams is difficult, because the heat flux measured on the wall q_{test} consists of two parts: the heat flux transferred by the particles and the heat flux from the gas in the presence of the particles. Thus

$$q_{\text{test}} = (\alpha/c_p)_\Sigma (H_e - h_w) + q_s = q_\Sigma + q_s. \quad (1)$$

The heat flux from the particles that have arrived at the surface of a body can be expressed in terms of their energies and flow rate G_{pw} in the form [1-3]

$$q_s = K_a G_{\text{pw}} \left[\frac{V_{\text{pw}}^2}{2} + c (T_p - T_w) \right]. \quad (2)$$

The coefficient of thermal energy accommodation for the particles K_a allows for the fact that during the impact the particles may have no time to give off their entire energy to the exposed surface; the coefficient depends on the phase state of the particles, the presence of a melt film or roughness on the surface, the angle of attack, and many other factors.

Within the ranges of velocities of the heterogeneous-stream gas component 900–2500 m/sec and sizes of the particles 100–200 μm , it was found that on the surface of a titanium model $K_a \approx 0.7$. In other investigations on models made of nonmetallic materials values of K_a of the order of 0.3 were obtained.

The influence of particles suspended in a stream on the transition of a laminar boundary layer into a turbulent one is also ambiguous. It has been established that small-sized particles (up to 50 μm) exert virtually no

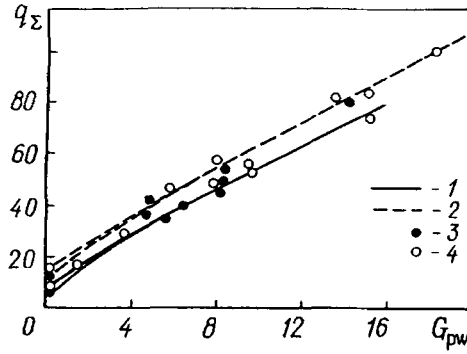


Fig. 1. Dependence of heat fluxes on the density of the mass flux of particles of size $d_p = 100 \mu\text{m}$: 1) model with a plane end face; 2) hemispherically blunted model; 3) radius of the model is 40 mm; 4) 20 mm. q_Σ , MW/m^2 , G_{pw} , $\text{kg}/(\text{m}^2 \cdot \text{sec})$.

effect on the boundary-layer transition. Larger particles reduce the critical Reynolds number, and, with increase in concentration, this reduction is more substantial, because the trace formed by a particle becomes turbulent.

A theoretical model of heat exchange in the vicinity of the stagnation point of a blunt body was based on several hypotheses that were subsequently refined by analyzing results of tests [15, 16].

It was assumed that the increase in the convective heat flux q_Σ relative to the corresponding value q_0 in a homogeneous stream, or the difference $\Delta q = q_\Sigma - q_0$, is attributable to the change in the flow field in the boundary layer made by the particles. The thickness of this layer is

$$\delta = Ax/\sqrt{\text{Re}_x} = A \sqrt{\eta_2/(\rho_2 \beta)},$$

where $\beta = (du_e/dx)_{x=0}$ is the flow-velocity gradient at the front stagnation point; the dimensionless coefficient A , which takes into account the effect of the compressibility and temperature factor of the stream lies within $4.4 \leq A \leq 5.7$ for the conditions of the tests.

The theoretical model assumes that the increment of the convective heat flux is a linear function of the kinetic energy of the particles:

$$\Delta q = q_\Sigma - q_0 = \psi \rho_\delta V_{pw}^3, \quad (3)$$

where ρ_δ is the mass of the particles per unit volume of the wall layer. This relation does not allow for the difference between the temperatures of the particles T_p and the surface of the body immersed in the stream T_w , since the change in the kinetic energy in a supersonic stream greatly exceeds the change in the internal energy of the particles.

Due to the inertia of the particles in the vicinity of the stagnation point, $u_p \ll u_e$. This allows one to obtain an analytical solution for the equation of motion of the particles in the form [3]

$$u_p = \sqrt{\left(\frac{C_D \rho_2 x}{2 \rho_p d_p} \right)} (\beta x). \quad (4)$$

Correspondingly, the increment of the heat flux $\Delta q = q_\Sigma - q_0$ due to the presence of inertial particles in the boundary layer is proportional to the following combination of determining parameters:

$$\Delta q = \psi \left[\frac{G_p V_{pw}^3 \sqrt{d_p} \sqrt{\varphi_N}}{A \sqrt{x/R_N}} \sqrt{\left(\frac{\rho_p}{C_D \eta_2 a_*} \right)} \right]. \quad (5)$$

The degree of enhancement of heat exchange is associated primarily with the inertia of a particle and with the ability of the gas in the boundary layer to carry the particle away from the point of contact. The larger the

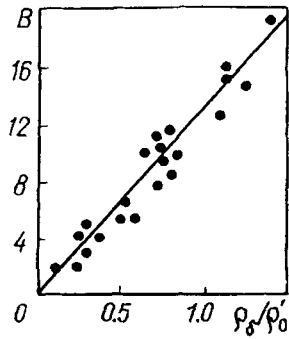


Fig. 2. Correlation for enhancement of heat exchange at the stagnation point of models immersed in a heterogeneous stream, $B = [(\Delta q RT_0') / (q_0 R_N^{0.5} V_{pw}^3 (\rho_0')^{0.75})] \cdot 10^8$.

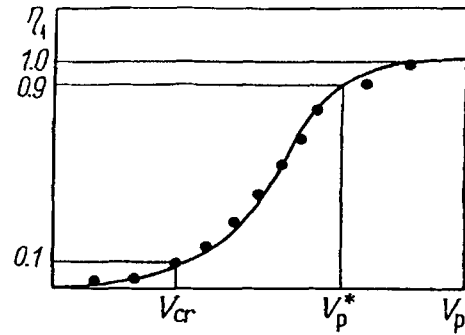


Fig. 3. A typical form of the change in the parameter η_1 with the velocity V_p , m/sec.

diameter of the particles, the deeper the mass of high-temperature gas penetrates the wall layer, and the larger the local volumes of the perturbed stream.

When a body is immersed in a heterogeneous stream, in all the cases the maximum of the heat flux is located at the stagnation point, in contrast to homogeneous streams.

According to experimental data, the effect of the size and shape of a body in a stream on the enhancement of heat exchange Δq can be considered to be relatively moderate (see Fig. 1). Thus, a twofold increase in the radius of a sphere had little effect on the value of Δq (or q_Σ) at $G_p = 10 \text{ kg}/(\text{m}^2 \cdot \text{sec})$, which corresponds to an admixture concentration $z_p = 0.66\%$. The effect of the shape on heat exchange is more substantial, but it reduces to the coefficient of proportionality in the dependence of q_Σ on G_p . The theoretical model attributes this effect to differences in the velocity gradient β ; on a plane end face the value of β is 2.3 times smaller than on a hemisphere; this also reduces the ventilating ability of the stream in the boundary layer.

To make theory (5) consistent with experiment, correlation of all the experimental data was carried out (Fig. 2). It is seen that in generalized coordinates the experiment is described well by a linear function. This made it possible to determine the coefficient of proportionality in formula (5) as $\psi = 1.3 \cdot 10^{-7}$.

The problem of the collision of deformed bodies, like any other physical problem, has relatively simple solutions in certain asymptotic cases. One of these is the range of impact velocities $10^3 - 5 \cdot 10^3 \text{ m/sec}$, when, according to experimental data, the depth of the crater left on impact of a single particle and the mass entrained are proportional to the kinetic energy of the striker. In this relation, the coefficient of proportionality was called the effective enthalpy of erosion H_{er} . It is a certain physical characteristic of the barrier material.

When the velocity is much smaller than 10^3 m/sec , all the parameters of the process of erosion change in a rather complicated fashion, with the difference being due not only to the material of the barrier, but also to the material of the striker itself.

The impact velocity V_p has a strong effect on the intensity of steady erosion \bar{G} . Using the energy conservation law, we have

$$\eta_1 \left(m_p \frac{V_p^2}{2} \right) = m_{er} H_{er} \quad \text{or} \quad \bar{G} = \eta_1 \frac{V_p^2}{2H_{er}}. \quad (6)$$

Here, two new parameters are introduced: H_{er} is the effective enthalpy of erosion and η_1 is the coefficient of conversion of the kinetic energy of collision of particles into the energy of destruction of the barrier material.

It is evident that the coefficient η_1 must depend on the impact velocity V_p . The smaller the velocity, the larger the portion of the kinetic energy of a particle that has time to scatter in the form of the energy of rigid vibrations in the barrier and eventually to transform into heat. Conversely, at a large velocity V_p the processes of destruction prevail over dissipation of energy in the undamaged portion of the barrier material. The dependence

of η_1 on V_p has an asymptotic character (Fig. 3). We can isolate the entire velocity range (V_{cr} , V_p^*) of change in the coefficient η . If we assume that $0.1 \leq \eta_1 \leq 0.9$, then, according to experimental data, the following approximate equality is obtained for a number of materials [9-11]:

$$V_p^* \approx 2V_{cr}. \quad (7)$$

The value of the velocity V_{cr} can be adopted as an arbitrary limit of the beginning of erosion.

Thus, when the impact velocity $V_p < V_{cr}$, elastoplastic deformation of the material occurs without mass entrainment. Within the range $V_{cr} < V_p < V_p^*$ the strength characteristics of the material still exert their effect on the intensity of destruction. And finally, when $V_p > V_p^*$, the so-called hydrodynamic mechanism of erosion develops. In this case the single parameter that evaluates the intensity of the process is the effective enthalpy of destruction H_{er} :

$$H_{er} = V_p^2 / (2\bar{G}). \quad (8)$$

Similarly to the heat of fusion, this enthalpy does not depend on the level of the energy effect (more precisely, on the impact velocity V_p). However, the effective enthalpy H_{er} is a more complex parameter than the heat of fusion, since H_{er} depends on both the structure of the material and other properties of the particle and the barrier.

The effects of fluxes of particles and a single particle differ both quantitatively and qualitatively. The energy parameter that determines this difference is the kinetic energy of the flux of particles that precipitate onto the exposed surface of the body. It was found from experimental data [6] that there is a definite value of the kinetic energy $(m_p^* V_p^2) / 2 = a^*$, above which the process of destruction seems to stabilize. Figure 4 shows that for all particles with dimension smaller than some threshold value

$$d_p < d_p^* = 3a^* / \rho_p V_p^2,$$

the effective enthalpy $H_{er}(1)$ turns out to be higher than the stationary value of H_{er} . This indicates a proportional decrease in the damage to the barrier or the dimensions of the crater.

For any prescribed impact velocity V_p the value of d_p^* divides the entire set of particles into two regions: small particles, for which the scale effect is important, and large particles, where all the processes of erosion are independent of the size of the particles.

Since the critical velocity is proportional to the effective enthalpy of destruction, while the difference between the effective enthalpies can be very appreciable for single and group impacts of particles, it is necessary to distinguish between the critical velocity of the stationary process of destruction in a flux of particles V_{cr} and the critical velocity of destruction caused by a single small particle $V_{cr}(1)$:

$$\frac{V_{cr}(1)}{V_{cr}} = \sqrt{\left(\frac{H_{er}(1)}{H_{er}}\right)} = \frac{1}{V_p} \sqrt{\left(\frac{3a^*}{\rho_p d_p}\right)}, \quad d_p < d_p^*.$$

Equating V_p and $V_{cr}(1)$ in this relation, we obtain

$$V_{cr}(1) = (V_{cr})^{0.5} \left(\frac{3a^*}{\rho_p d_p}\right)^{0.25}. \quad (9)$$

The change in the critical velocity of the "beginning of erosion" $V_{cr}(1)$ with increase in the diameter of the particles in proportion to $(d_p)^{-0.25}$ determines the importance of the scale effect and furnishes an indirect check of the entire physical model of the process. Despite a lack of experimental data, the agreement between the calculated and experimental data can be considered quite satisfactory [2, 3].

A substantial change in H_{er} is possible at high heat load. A measure for comparison of the intensity of the thermal and erosional effect is the mean integral temperature T_s , which takes into account the rate of both erosion

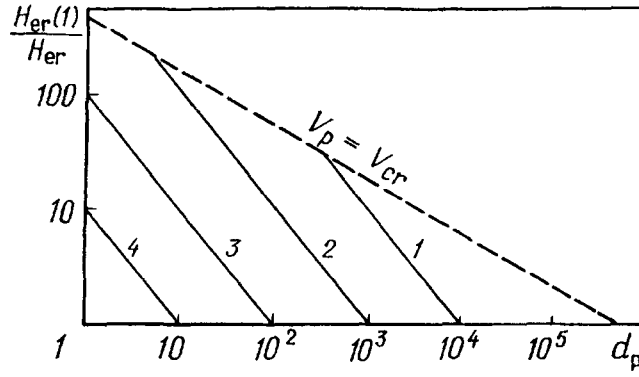


Fig. 4. Effect of the size of the particles d_p on the difference between the effective enthalpies of erosion for a single impact $H_{er}(1)$ and for a developed process of destruction H_{er} ($\rho_p = 3600 \text{ kg/m}^3$): 1) $V_p = 300 \text{ m/sec}$, 2) 1000, 3) 3000, 4) 10,000. $d_p, \mu\text{m}$.

and thermochemical destruction, the depth of the crater and, consequently, the size of the particles, and thermophysical and other parameters of the barrier material:

$$T_s = \frac{1}{h} \int_0^h T(y) dy.$$

In the case of quasistationary destruction, the function $T_s(h)$ has the following form:

$$\theta_s = \frac{T_s - T_0}{T_w - T_0} = \frac{\lambda_0}{hc_0 G_\Sigma} \left[1 - \exp\left(-\frac{hc_0 G_\Sigma}{\lambda_0}\right) \right]. \quad (10)$$

Comparing the linear rate of erosion (h/τ_{er}) and the parameter that characterizes the velocity of thermal-wave propagation in the barrier material (δ_T/τ_T), a criterion of thermal similarity for the thermal-erosional effect of a heterogeneous stream was obtained that makes it possible to assess the mean integral temperature over the entire range of the depths of the craters. It turned out that the criterion is a product of time and space scales and is equal to [1, 7, 8]

$$E = \frac{h\pi_T}{\delta_T\tau_{er}} = \left[\frac{G_p V_{pw}^2}{2q_\Sigma} \right]^2 \left[\frac{c_0 (T_w - T_0)}{H_{er}} \right]^2 \left(\frac{G_t}{G_{er}} + 1 \right). \quad (11)$$

From the physical point of view, this fundamental energy criterion is the ratio of the amount of thermal energy in a surface layer of thickness h , scattered due to erosion, to the amount of thermal energy accumulated in the heated layer δ_T .

The processing of numerous results of experimental and computational investigations (Fig. 5) made it possible to establish a unified dependence of the dimensionless mean-integral temperature θ_s on the criterion E in the form of the relation

$$\theta_s = \frac{T_s - T_0}{T_w - T_0} = \exp(-0.1342E - 1.2787E^2 + 0.906E^3 - 0.2E^4). \quad (12)$$

Relation (12) allows one to evaluate the mean integral temperature T_s from the results of experimental investigations. The value $E^* \approx 1$ separates Fig. 5 into two regions characteristic for the thermal-erosional ($E < E^*$) and purely erosional ($E > E^*$) mechanisms of destruction. In the latter case the thermal component of mass entrainment can be neglected ($G_t \ll G_{er}$).

2. The Possibilities for the Use of Heterogeneous Streams in Modern Technologies. The fundamental distinction of heterogeneous streams from homogeneous ones consists in the existence of local mass concentrators.

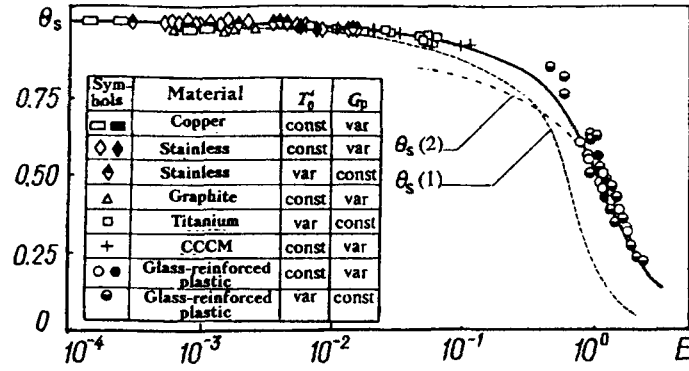


Fig. 5. Dependence of the dimensionless mean integral temperature of the surface layer of materials on the criterion E , Light symbols, results of testing materials at a stagnation pressure of 1.2 MPa; dark symbols, at 8.0 MPa; solid line, according to formula of (12).

In planetology such phenomena are called "mascons" (mass concentrations). Withdrawing energy from the carrier medium, they create extreme high levels of the energy effect on bodies immersed in them. It is also no less important that varying the size of the particles and their slip velocity relative to the gas, it is possible to attain a manifold change in the intensity of the heat exchange between two components of a heterogeneous medium. Thus, heterogeneity substantially increases the number of degrees of freedom in the system that controls the energy and force parameters in a particular technology. Among these, we may first of all mention devices for the cutting and sputtering of substances [4, 5, 7, 14, 17-20].

The shock-wave character of the loading and multiplication of the effect distinguish the operation of a supersonic heterogeneous cutter (SHC) from all other means of mechanical disintegration of a body. It is important that in this case the thermal effect is reduced to a minimum, and the cracks and spalls have a depth not exceeding the size of the particles introduced into the heterogeneous stream.

Creation of SHCs became possible only after knowledge of the fundamental processes of the interaction of the phases in heterogeneous systems had been gained. The apparent ease of implementation (of the sand-blast type) is very deceptive in reality. The efficiency of the process of cutting depends strongly on the velocity and mass of the impacting particles. It has been shown that only supersonic heterogeneous cutters can compete successfully with other similar devices. Therefore, optimization of the regime of the acceleration of particles in a gas flow is a serious scientific and engineering problem. It is reduced to the solution of a variational problem that determines the function $\lambda(V_p)$ with which the functional [2]

$$(x - x_0) = \int_0^{V_p} F[V_p, \lambda(V_p)] = dV_p \quad (13)$$

has an extremum. The Euler equation for an extremum will be written as

$$\frac{2\bar{V}_p}{(\lambda - \bar{V}_p)^3} \left(1 - \frac{k-1}{k+1} \lambda^2\right)^{-\frac{1}{k-1}} \left[1 - \frac{\lambda(\lambda - \bar{V}_p)}{k+1} \left(1 - \frac{k-1}{k+1} \lambda^2\right)^{-1}\right] = 0. \quad (14)$$

This equality holds only in the case where the expression in square brackets vanishes, so that

$$\bar{V}_p = k\lambda - \frac{k+1}{\lambda}. \quad (15)$$

Thus, the shape of an optimum nozzle can be calculated using Eq. (15).

We will note one specific feature of the solution obtained for the variational problem. From condition (15) it follows that gas can attain the greatest acceleration in the section of the flow where the particles are mixed with gas whose velocity $\lambda \geq \sqrt{(k+1)k}$. In other words, an optimum nozzle for accelerating a heterogeneous mixture is

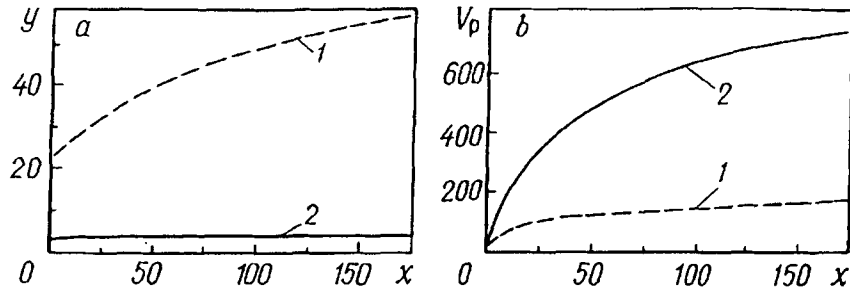


Fig. 6. Profiles of nozzles at $p_{00} = 5$ MPa (a) and velocities of particles (b) in a standard nozzle (1) and in a nozzle optimized for SiO_2 particles of size $d_p = 100 \mu\text{m}$ (2). y, x , mm; V_p , m/sec.

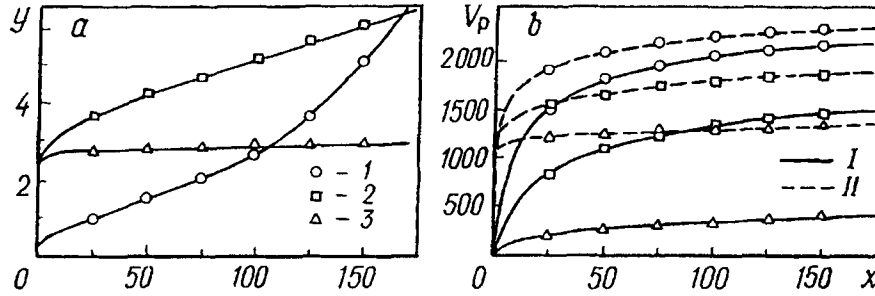


Fig. 7. Profiles of optimized nozzles for acceleration of SiO_2 particles (a) and velocities of acceleration of SiO_2 particles (I) and gas (II) in them (b) for the parameters in the prechamber $p_{00} = 2$ MPa and $T_0 = 2350$ K: 1) size of the particles $d_p = 3 \mu\text{m}$, 2) 10, 3) 200.

supersonic everywhere. This does not mean that the subsonic part of the nozzle cannot be used to place in it a system for the supply of the particles. However, the role of this part consists not so much in the acceleration of particles, as in the uniform seeding of the entire gasdynamic circuit with them. There is a danger, of course, that in high-temperature gas generators the particles may be overheated and crushed. In this regard, it is advisable to decrease as much as possible the residence time of the particles in the subsonic part of the nozzle.

To illustrate the efficiency of the method used to optimize the nozzle of a heterogeneous cutter, we present below results of numerical calculations. It is assumed that the particles are spheres with a diameter d_p from 3 to 200 μm , the pressure in the gas generator varies from 2 to 20 MPa, and the temperature corresponds to the stoichiometric temperature of the burning of kerosene in air.

Figure 6a compares the geometries of the supersonic parts of a classical Laval nozzle and an optimum nozzle, and Fig. 6b presents data on the dynamics of the increase in the velocity V_p for particles with $d_p = 100 \mu\text{m}$ and $p_{00} = 5$ MPa. It is seen that even on a nozzle length of 170 mm silicon oxide particles could not be accelerated in the Laval nozzle to a velocity of 200 m/sec, whereas in the optimum nozzle their velocity was four times higher. In Fig. 7, the size of the particles is varied (from 3 to 200 μm) for the same pressure in the prechamber of the facility $p_{00} = 2$ MPa. It is seen that the larger the particles, the closer the profile of the optimum nozzle is to a cylindrical one (Fig. 7a) and the more slowly the particles gain velocity. The velocity lag of the particles $\varphi_L = (V - V_p)/V$ on the length $L = 170$ mm decreases from 0.66 for particles with $d_p = 200 \mu\text{m}$ to 0.06 for $d_p = 3 \mu\text{m}$. According to Eq. (15), the velocity of the carrier medium at the tip of the optimum nozzle turns out to be different too (from $\lambda_L = 1.5$ for large particles to $\lambda_L = 2.5$ for the smallest ones): $\lambda_L \approx \sqrt{(k+1)/[\varphi_L + (k-1)]}$.

This cycle of calculations allowed one to recommend the relation $[(\rho_{00}/\rho_p) (L/d_p)] \geq 20$ for evaluating the parameters of the cutter, which makes it possible to calculate from below either the length of the nozzle L for a fixed pressure p_{00} or the pressure in the prechamber of the cutter for a prescribed length of the nozzle.

In practice the particles may differ strongly in shape and size. Their motion in a gas stream already cannot be described within the framework of any theoretical model of optimization, since one profile of a nozzle is required for small particles and another for large particles. Nevertheless, here too some techniques have been developed that

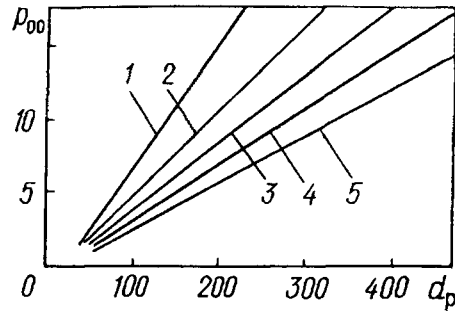


Fig. 8. Optimum operational parameters of a supersonic heterogeneous cutter in relation to the depth of cutting h_c : 1) $h_c = 20$ mm, 2) 40, 3) 60, 4) 80, 5) 100 mm. p_{00} , MPa.

sharply increase the efficiency of gas-dust cutting. They are associated with equalization of the velocity field at the tip of the optimized nozzle. To equalize the velocity of the particles in a polydisperse stream, a section with a constant value of the gas velocity V (or λ) over the length is required. Then the scatter in the velocities of particles of different sizes will be reduced, and the velocity of the particles lagging behind will tend to approach the gas velocity.

A nozzle channel that ensures acceleration of a polydisperse heterogeneous stream should consist of two parts. Over the first part the most representative fraction of the particles moves under extreme conditions of aerodynamic interaction with the stream, due to which the accelerating length of the nozzle is decreased. Over the second part the velocities of all the remaining fractions of the particles equalize.

The data obtained made it possible to carry out optimization of the regime of operation of a gas-dust cutter, which was reduced to determination of the extremum in the kinetic energy of the particles as a function of the pressure in the prechamber of the facility and the size of the particles. As a result it turned out that the kinetic energy of the stream of particles under extreme conditions on a bench depends little on either the pressure in the prechamber of the facility or the size of the particles. It should be kept in mind in this case that each dependence on the pressure corresponds to its own size of the particles and conversely: each value of the size of the particles corresponds to a certain pressure. Dependences of the optimum pressure that should be maintained in the prechamber of the facility in order that the flux of particles of prescribed size have the maximum kinetic energy are presented in Fig. 8.

In recent decades new gasdynamic methods of creating structural materials and coatings have been widely applied in industry: the plasma and gas-flame, detonation, electric-arc, and other techniques. However, despite the simplicity and mobility of these methods, they have a number of important drawbacks due, first of all, to the use of a high-temperature (several hundred or thousand degrees) gas jet that has a low velocity and high chemical corrosiveness. The latter exerts an irreversible negative effect on the initial components of the coating produced and, as a consequence, impairs its quality. This is explained by the low velocity of the two-phase stream, as well as by the presence of intense homogeneous and heterogeneous chemical reactions that are inadmissible in a number of cases in the technological process of formation of the coating. To remedy the situation, the plasma method, for example, uses costly inert gases (argon, helium, xenon, etc.), which makes implementation of the method more expensive. Moreover, the creation of a high-temperature jet requires high levels of electric power.

A logical development in both the plasma and gas-flame method is the cold gasdynamic method (CGDM) of sputtering developed at the Moscow Aviation Institute at the beginning of the 1990s [12, 13]. The essence of the method is that materials and coatings are synthesized as a result of impact of high-velocity heterogeneous streams against a substrate. The material is composed of a number of chemical elements or compounds (metals, oxides, carbides, nitrides, etc.) needed to obtain the desired properties, made in the form of powders with a dispersity of from 10 to 50 μm . The needed spectrum of diverse powders composed in the corresponding mass fractions is preliminarily mixed in a special gasdynamic mixer. The preparation obtained in this way is accelerated in a supersonic nozzle to the calculated (for the given composition) velocity providing the particles with a high kinetic energy, which is converted to thermal energy upon their impact against the substrate.

TABLE 1. Values of the Microhardness of the Initial Powder Materials and Coatings Synthesized from Them

Element	Microhardness, MPa		Ratio of microhardnesses, %
	of initial material	of coating	
Zn	400	650	162
Al	300	550	183
Cu	600	1000	167
Cr	1150	2900	252
Fe	750	2100	280
Ni	1150	1800	156
Co	1150	3200	243

TABLE 2. Microhardness of Gasdynamic Coatings after Annealing at Different Temperatures for One Hour, MPa

Element	Temperature, °C									
	0	100	200	300	400	500	700	800	900	1000
Zn	650	650	650	650	—	—	—	—	—	—
Al	550	550	550	550	550	550	—	—	—	—
Cu	1000	1000	1000	1000	1000	1000	1000	1000	1000	—
Cr	2900	2900	2900	2900	2900	2900	2900	2900	2900	2900
Fe	2100	2100	2100	2100	2100	2100	2100	2100	2100	2100
Ni	1800	1800	1800	1800	1800	1800	1800	1800	1800	1800
Co	3200	3200	3200	3200	3200	3200	3200	3200	3200	3200

One of the most important advantages of the CGDM of sputtering in comparison with other hot-gas methods (plasma, electric-arc, gas-flame, detonation) is the fact that the material is synthesized owing to the high level of the kinetic energy of the particles, whereas the temperature of the stream remains much below their melting temperature. This excludes physicochemical transformations and oxidation of the powder material, and the particles reach the substrate in their initial state, which makes it possible to use inexpensive technical air as the carrier gas.

Based on the CGDM of sputtering, a circuit was designed and a laboratory setup was developed. Preliminary investigations revealed a number of very important scientific aspects that ensure broad possibilities for the method. Thus, it was found that high-velocity impact of particles against a substrate leads to mutual plastic deformation and activation of the surface owing to a high local pressure at the spot of contact. As a result of shock-wave loads appearing both in the particles and on the surface of the substrate, as well as of dissipation of kinetic energy, which is converted into thermal energy at the moment of impact with localization of the temperature peak, physicochemical and phase conversions occur at the spot of impact both between the substrate and the first coating layer and in subsequent layers and the bulk of the material. Such conversions have been identified, for example, in the Cu–Zn, Ni–Al, Co–Al systems both in the interaction of Zn, Ni, Co particles with copper and aluminum substrates and in Cu and Zn, Ni and Al, Co and Al mixed powders taken in the corresponding proportions. In the first case, intermetallic compounds are formed in the transition zone (for example, in the form of brass, Cu+Zn), and in the second case intermetallides are formed in the bulk of the layer, forming a new material – Cu+Zn. It is natural to assume that the properties of this material are determined by both the mass concentrations of the composite powder and the parameters of the particles and their energy and size.

The collection of the characteristics detected even at the level of preliminary investigations allow one to assert that the CGDM of sputtering may be used to create various composite materials, to program their properties, to control the technological process with a high degree of accuracy, and to monitor it to attain complete

environmental safety. Moreover, the CGDM is much less expensive than the traditional methods. The CGDM of sputtering will make it possible to realize superfaster technologies that do not require considerable energy expenditures. For example, to obtain a 1-mm-thick layer of the intermetallide NiAl on a 10-mm-diameter spot by using the CGDM, several tenths of a second is needed, whereas in the standard technology a 60- μm -thick transition zone is formed in furnaces in 9 h at a temperature of 970 K.

The CGDM of sputtering allows one also to synthesize metal-ceramic materials, with their formation being realized owing not only to the increase in the velocity of the particles, but also to the developed efficient technology for introducing, in the process of material synthesis, additional energy and exothermic reactions occurring in the process of interaction of high-velocity particles with the substrate.

The use of such a technique makes it possible to form coatings of carbides, borides, oxides, silicides, and other refractory compounds on a substrate. For example, using the CGDM and the corresponding insignificant amounts of admixture, it was possible to synthesize the following reactions on a substrate: $\text{B}_4\text{C} + 3\text{Ti} = 2\text{TiB}_2 + \text{TiC}$, $3\text{SiC} + 8\text{Ti} = \text{Ti}_5\text{Si}_3 + 3\text{TiC}$, $\text{Nb} + \text{C} = \text{NbC}$.

The types of metal-ceramics produced can find wide application in new technologies owing to their high thermal and mechanical properties. In the set of the discovered processes that accompany the synthesis of materials by the CGDM a number of features have been revealed whose investigation may open up still greater scientific and practical possibilities for the method. Thus, for example, a preliminary investigation of the microhardness of coatings synthesized on a surface showed its considerable increase compared to the microhardness of the initial material of the powder (Table 1):

In this case, attention should be paid to the fact that the higher hardness of the synthesized materials is also preserved after prolonged annealing of them at temperatures that exceed the recrystallization temperature of the elements. Results of experiments are presented in Table 2. Use of this phenomenon opens up broad possibilities for creating new types of materials with prescribed properties.

The work was carried out under financial support from the Russian Fundamental Research Fund (grant No. 97-02-16649).

NOTATION

α , heat-exchange coefficient; β , velocity gradient of the stream on the outer edge of the boundary layer; δ , boundary-layer thickness; δ_T , characteristic scale of the heated layer; $\Delta q = q_\Sigma - q_0$, increment of convective heat flux in the heterogeneous medium compared to the homogeneous one; η , η_1 , gas viscosity and coefficient of transformation of the kinetic energy of the stream of particles into the energy of barrier destruction, respectively; φ_L , relative slip velocity of the phases; φ_N , shape factor of a blunt body; λ_0 , thermal conductivity of the barrier material; λ , dimensionless coefficient of the gas stream velocity, $\lambda = V/a_*$; ρ_{00} , ρ_2 , gas density in the prechamber for the stagnation flow and flow behind the shock wave; ρ_δ , distribution density of the particles in the bulk of the wall layer; ρ_p , density of the particles; τ_T , τ_{er} , characteristic scales of heating and erosion; A , proportionality constant in the function $\delta(\text{Re})$; a_* , speed of sound in the critical cross section ($M = 1$); a^* , threshold value of the kinetic energy of the particles; c , c_p , heat capacity of the particles and heat capacity of the gas at constant pressure, respectively; C_D , coefficient of aerodynamic drag of the particles; d_p , diameter of the particles; E , energy criterion of thermal-erosional destruction; η_2 , dimensionless coordinate along the boundary-layer thickness in the standard Blasius relation; G_p , mass flux of particles on the barrier surface; G_t , G_{er} , $G_\Sigma = G_{er} + G_t$, velocity of mass entrainment in thermal and erosional destruction; \bar{G} , dimensionless rate of impact-induced erosion; h , h_c , depth of the crater and the slit cut in the barrier, respectively; H_e , h_w , total and thermodynamic enthalpies of the gas in the boundary layer; K_a , coefficient of thermal accommodation of the kinetic energy of the particles; K , specific-heat ratio; L , length of the nozzle block of the cutter; m_{er} , mass of the barrier entrained due to erosion; m_p , mass of a the particle; m_p^* , threshold value of the mass of particles at the moment of development of erosion; p_{00} , p'_0 , pressure in the prechamber and stagnation-flow pressure; q_{1est} , q_s , q_Σ , components of the heat flux on the barrier surface in the heterogeneous stream; Re_x , Reynolds number; R_N , radius of curvature at the critical point of the bluntness; T_p , T_w , temperatures of the particles and the barrier surface; T_s , mean integral value of the temperature along the

value of the temperature along the depth of the crater; V_p , V_{pw} , velocity of particles in the gas stream, at the nozzle outlet, and upon impact against the barrier; V_{cr} , V_p^* , velocity of the particles at the beginning of the process of destruction and upon its development (threshold value); x , y , coordinates; z_p , mass concentration of the particles in the stream; u_e , gas velocity at the edge of the boundary layer; u_p , velocity of the particles; CCCM, carbon-carbon composite material.

REFERENCES

1. A. V. Vasin and Yu. V. Polezhaev, *Izv. Akad. Nauk SSSR, Mekh. Zhidk. Gaza*, No. 1, 120-126 (1984).
2. D. S. Mikhatulin and Yu. V. Polezhaev, *Teplofiz., Vysok. Temp.*, 30, No. 2, 325-333 (1992).
3. D. S. Mikhatulin, Yu. V. Polezhaev, and I. V. Repin, *Heterogeneous Flows: Gas Dynamics, Heat Exchange, Erosion*, Preprint No. 2-402, IVTAN, Moscow (1997).
4. P. Nikitin, "Methode Gazodinamique pour l'Elaboration de Nouveaux Materiaux Composites et de Revetements Multifunctions," in: France-Russia Scientific Conference "Nouveaux Materiaux Composites," Laboratories SEP Vernon, France, December (1993).
5. Yu. V. Dikun, P. V. Nikitin, and Yu. P. Frolov, "Algorithm for calculation of two-phase flows with allowance for friction and heat exchange," in: *Proceeding of the Scientific-Engineering Seminar with Participation of the SEP Company*, France, MAI, Moscow (1994), pp. 20-23.
6. Yu. V. Polezhaev, *Inzh.-Fiz. Zh.*, 37, No. 3, 389-394 (1979).
7. Yu. V. Polezhaev and D. S. Mikhatulin, *Izv. Akad. Nauk SSSR, Mekh. Zhidk. Gaza*, No. 4, 92-98 (1986).
8. Yu. V. Polezhaev and D. S. Mikhatulin, *Izv. Akad. Nauk SSSR, Energet. Transp.*, No. 5, 36-48 (1991).
9. Yu. V. Polezhaev and V. I. Panchenko, *Inzh.-Fiz. Zh.*, 52, No. 5, 709-716 (1988).
10. Yu. V. Polezhaev, V. P. Romanchenkov, I. V. Chirkov, and V. N. Shebeko, *Inzh.-Fiz. Zh.*, 37, No. 3, 395-404 (1979).
11. Yu. V. Polezhaev and G. A. Frolov, *Inzh.-Fiz. Zh.*, 52, No. 3, 892-896 (1987).
12. Yu. V. Dikun, Yu. A. Kocherin, P. V. Nikitin, and Yu. P. Frolov, "A means of production of coatings," Positive decision on application No. 4946269/26/050925, cl. 5C23C24/04 of 17.06.1991.
13. P. V. Nikitin, Yu. V. Dikun, A. G. Smolin, I. I. BasalaeV, and G. V. AbramIn, "A device for applying coatings," Positive decision of the expertise commission of VNIIGPÉ on application No. 95109772/202/017/313, cl. 6C23C24/04 of 05.06.1995.
14. D. Mikhatulin and Yu. Polezhaev, "Methods and facilities for the simulation of heat transfer in high-velocity heterogeneous flow," in: *Aerosols: Science, Devices, Software and Technologies of the Former USSR*, Vol. 2, No. 1 (1996), pp. 35-36.
15. D. Mikhatulin, Yu. Polezhaev, and I. Repin, *Heat Transfer Research*, 25, No. 3, 356-360 (1993).
16. D. Mikhatulin, Yu. Polezhaev, and I. Repin, "Heat transfer in particle environments," in: *Heat and Mass Transfer-95, Proceedings of the 2nd ISHMT-ASME Heat and Mass Transfer Conference, 13th National Heat and Mass Transfer Conference*, India, Karatake, KREC (1995), pp. 429-433.
17. P. Nikitin, "Cold gasdynamic method for synthesis of composite materials and multifunctional coatings with predicted thermophysical characteristics," in: *Proceedings of the Int. Conf. on Fluid and Thermal Energy Conversion '94*, Denpasar, Bali, Indonesia (1994), pp. 152-156.
18. P. Nikitin, "Problem issues of development of thermal protection systems for spacecraft," in: *Papers presented at the 1st Int. Conf. on Aerospace Heat Exchanger Technology*, Palo Alto, California, February (1993).
19. P. Nikitin, "The thermal protection systems for spacecraft," in: *Proceedings of the 6th Int. Symp. on Transport Phenomena in Thermal Engineering (ISTP-6)*, Seoul, Korea (1993), pp. 141-146.
20. P. Nikitin, N. Andreev, and V. Paiko, "Cold gasdynamic method for synthesis of the new composite materials and multifunctional coatings with predicted thermophysical characteristics," in: *Proceedings of the 13th National Heat and Mass Transfer Conference*, India (1995), pp. 839-844.